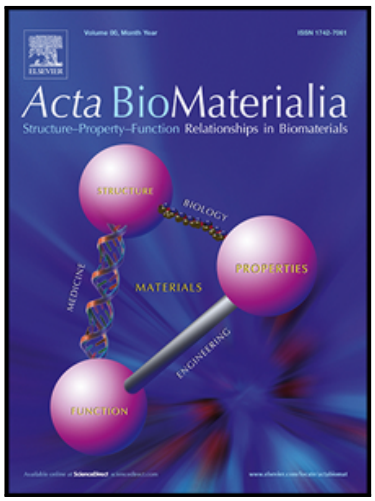

RHAMM expression tunes the response of breast cancer cell lines to hyaluronan

Ana M. Carvalho , Diana Soares da Costa , Rui L. Reis , Iva Pashkuleva

PII: S1742-7061(22)00282-3
DOI: https://doi.org/10.1016/j.actbio.2022.05.013
Reference: ACTBIO 8021

To appear in: *Acta Biomaterialia*

Received date: 28 January 2022
Revised date: 12 April 2022
Accepted date: 8 May 2022

Please cite this article as: Ana M. Carvalho , Diana Soares da Costa , Rui L. Reis , Iva Pashkuleva , RHAMM expression tunes the response of breast cancer cell lines to hyaluronan, *Acta Biomaterialia* (2022), doi: https://doi.org/10.1016/j.actbio.2022.05.013

RHAMM expression tunes the response of breast cancer cell lines to hyaluronan

Ana M. Carvalho[1,2], Diana Soares da Costa[1,2], Rui L. Reis[1,2] and Iva Pashkuleva[1,2,*]

[1] 3B's Research Group, I3Bs Research Institute on Biomaterials, Biodegradables and Biomimetics, University of Minho, Headquarters of the European Institute of Excellence on Tissue Engineering and Regenerative Medicine, 4805-017 Barco, Portugal

[2] ICVS/3B's – PT Government Associate Laboratory, University of Minho, Portugal

*pashkuleva@i3bs.uminho.pt

Abstract

Hyaluronan (HA) synthesis and degradation are altered during carcinogenesis leading to an increased HA content in the tumor microenvironment, which correlates with poor prognosis and treatment outcomes. The main HA receptors, CD44 and RHAMM, are also overexpressed in tumors where they activate anti-apoptotic, proliferative, invasive, and migration signaling pathways.

Herein, we used a unidirectional HA gradient to investigate in a high-throughput fashion the bi-directional communication between HA and breast cancer cell lines with different surface expression of CD44 and RHAMM. We found that the expression of CD44 and RHAMM depends on the HA density: the expression of these receptors is promoted at higher HA density and RHAMM is more sensitive to these changes when compared to CD44. Blocking either CD44 or RHAMM revealed different functions on binding and recognizing HA and a compensatory expression between these two receptors that maintains protumorigenic effectors such as cortactin.

Statement of Significance We show that the expression of main hyaluronan (HA) receptors CD44 and RHAMM is enhanced in a HA concentration-dependent manner. Blocking activity experiments with either RHAMM or CD44 reveal the redundancy of these two receptors towards HA recognition

and activation/recruitment of protumorigenic molecular effector, cortactin. These experiments also demonstrate that cells with overexpressed RHAMM are more sensitive to HA density than CD44 positive cells. The reported results are important for the development of therapies that target the hyaluronan signaling in the tumor microenvironment.

Keywords

Breast Cancer, Hyaluronan, CD44, RHAMM, Compensatory Mechanism

1. Introduction

Breast cancer development and progression are correlated with a constant remodeling of the extracellular matrix (ECM). Among different ECM components, hyaluronan (HA) has been associated with several tumorigenesis processes.[1] Overexpression of hyaluronan synthases (HAS), particularly HAS2, leads to an accumulation of HA at the tumor site.[2-4] The increased content of HA is a poor prognosis marker of most invasive breast cancer cells because in the tumor microenvironment HA activates anti-apoptotic, pro-invasion, and pro-migration signaling pathways and regulates multidrug resistance, tumor growth, and progression.[5-11]

In breast cancer, HA bioactivity is transduced by its main receptors, cluster of differentiation 44 (CD44) and the receptor for hyaluronan mediated motility (RHAMM). CD44 is a type I transmembrane protein that interacts with HA *via* an amino-terminal link domain present at the protein ectodomain and common to other hyaladherins.[12, 13] This receptor is ubiquitously expressed at the cell surface, and it is involved in cell-cell and cell-ECM communication.[1] CD44 receptor is overexpressed in several cancers, including breast, and correlates with an aggressive behavior and poor prognosis.[14, 15] RHAMM binds HA through an HA-binding region that structurally differs from the CD44 one.[16] RHAMM has different cellular functions according to its localization in the cell: it can take part of the cell in-out signal transduction when is expressed at the

cell surface, and/or act as an intracellular effector and regulator of motile and proliferative pathways.[17-21] This HA receptor is not detected in most tissues; however, it is expressed during wound repair and in several cancers.[22] In breast cancer, RHAMM overexpression is linked to poor clinical outcomes.[23] Despite their structural differences, CD44 and RHAMM have some overlapping functions in HA signaling, and both compensatory and cooperative mechanisms between these receptors have been proposed.[5, 24-26] Herein, we developed molecular gradients to study the relationship between HA content and CD44 and RHAMM expression and function.

2. Materials and Methods:

2.1 Materials. Sodium hyaluronate (HA, weight average molecular weight (MW), 4.8 kDa, MW dispersity of 1.2) was acquired from Lifecore (USA). End-on-thiolated HA was synthesized by coupling a short (C_{11}) alkanethiol at HA reducing end using an oxime reaction, as previously described (details provided in the SI).[5, 27] The antibodies used in this study were monoclonal antibody to CD44 – Ascites (Acris), anti-CD44 antibody [KM201] (Abcam), anti-CD168 antibody [EPR4055] (Abcam), RHAMM antibody (H-8) (Santa Cruz Biotechnology), anti-CD44-PE (BD Biosciences), and AlexaFluor® 594 donkey anti-mouse IgG1 (H+L) (ThermoFisher Scientific). We used 4′,6-diamidino-2-phenylindole (DAPI, Biotium), and fluorescein isothiocyanate labeled phalloidin (phalloidin-FITC, Sigma) for nucleus and cytoskeleton staining, respectively.

2.2 Preparation of HA gradients. Glass coverslips (2 x 2 cm^2) were cleaned in piranha solution and amino-functionalized using 3-(aminopropyl)triethoxysilane (APTES) (1% v/v in acetone, 30 min, room temperature (RT)). Substrates were washed with acetone in an ultrasonic bath and cured (110 °C for 1 h under vacuum).[28, 29] Gold nanoparticles were synthesized by the Turkevich method[30] (details provided in the SI) and immobilized on the amino-functionalized coverslips by diffusional deposition. Briefly, a dispersion of gold nanoparticles (5 mL of the obtained gold nanoparticles colloidal suspension in 95 mL of Milli-Q water) was pumped (100 mL/min for 2 h) at

the bottom of a container with the vertically positioned substrate. The generated gold nanoparticles gradients were washed with Milli-Q water, dried under nitrogen flow, and stored or further functionalized by immobilization of end-on-thiolated HA (0.5 mg/mL in Milli-Q water, overnight incubation, RT). The HA-functionalized substrates were washed with phosphate-buffered saline (PBS) and passivated with bovine serum albumin (BSA 3 % w/v in PBS for 30 min at RT). Wheat germ agglutinin (WGA) Alexa Fluor® 488 conjugate (1.25 μg/mL in PBS, 10 min, RT, Molecular Probes) was used to confirm the presence and bioactivity of the immobilized HA. Gold nanoparticles gradients passivated with BSA were used as a control substrate.

2.3 Breast cancer cells culture and interaction with HA gradients. The obtained gradients were sterilized with UV light (30 min) before cells seeding. We used two breast cancer cell lines, namely MDA-MB-231 and Sk-Br-3 (American Type Culture Collection, ATCC). Cells were kept in culture on tissue culture polystyrene in Dulbecco Modified Eagle Medium high glucose (4500 mg/L) containing phenol red (Sigma-Aldrich) and supplemented with 3.7 mg/mL sodium bicarbonate (Sigma-Aldrich), 10 % fetal bovine serum (FBS, Gibco) and 1 % antibiotic/antimycotic (10000 units/mL penicillin G sodium, 10000 μg/mL streptomycin sulfate, and 25 μg/mL amphotericin B in 0.85% saline; Gibco) at 37 °C with 5% CO_2 humidified atmosphere. At 80 % confluence, cells were detached with TrypLE Express (Gibco), centrifuged (300*g* for 5 min), and subcultured.

To study the interaction with gradients (HA or gold), cells were seeded at a density of 10^5 cells/cm^2. For blocking CD44 or RHAMM receptors, cells (2 x 10^5 cells) were suspended in 100 μL of complete growth medium containing anti-CD44 antibody (1 μg, KM201 Abcam) or anti-CD168 antibody (400 ng, EPR4055 Abcam), respectively for 30 min at 37 °C in 5 % CO_2 humidified atmosphere. After washing with PBS, cells were seeded on gradients at a density of 10^5 cells/cm^2. Receptors' expression was evaluated 24 h after the seeding by immunocytochemistry.

2.4 Flow cytometry. Upon 70 % of confluence, cells were detached by incubation with 4 mM ethylenediaminetetraacetic acid (EDTA, Sigma-Aldrich) in PBS pH 8 (Sigma-Aldrich) for 10 min at 37 ºC in 5% CO_2 humidified atmosphere. Cells were characterized by flow cytometry using the following antibodies: human anti-CD44 PE (BD Pharmingen) and RHAMM antibody (H-8) (Santa Cruz Biotechnology). The expression of surface receptors CD44 was quantified by incubating the cells with anti-CD44-PE (2 µg for 5 x 10^5 cells in 100 µL of PBS) for 30 min at RT. In the case of RHAMM, cells were first incubated with the RHAMM antibody (H-8) (2 µg for 5 x 10^5 cells in 100 µL of PBS) for 30 min at 4 °C. After washing, a second incubation was performed with donkey anti-mouse Alexa Fluor® 488 (1 µg, ThermoFisher). Cells were washed with PBS, centrifuged for 5 min at 300*g*, and suspended in acquisition buffer (1 % formalin in PBS) for flow cytometry analysis (BD FACSCalibur).

2.5 Immunocytochemistry. Substrates with the cultured cells were washed with PBS, fixed with 10 % formalin (1 h at 4 °C), and cells were permeabilized with 0.2 % triton-X-100/PBS (15 min at RT). Incubation with monoclonal CD44 antibody (dilution 1:400 in 1% BSA/PBS) or with anti-CD168 antibody (1:200 in 1% BSA/PBS) was performed overnight at 4 °C. After washing with PBS, secondary antibody Alexa Fluor® 488 or Alexa Fluor® 647 (dilution 1:750) was added together with DAPI (1 µg/mL) and phalloidin (50 ng/mL) for nucleus and actin counterstaining (1 h at RT). Microscope slides were mounted with VectaShield mounting medium (Vector Laboratories), and fluorescent tiled images were acquired edge-to-edge of the gradient on an inverted confocal microscope (TCS SP8, Leica Microsystems). Image post-processing was performed by ImageJ 1.53c. Tiled images were projected to the sum and sectioned in 10 positions along the gradient. To quantify the mean grey value of CD44 and RHAMM, a region of interest (cell body, ROI) was first selected using the phalloidin signal. The ROI was then used to measure the mean grey value of the receptors signal. The number of adhesion cells was determined by nucleus counting.

2.6 Scanning Electron Microscopy (SEM). Substrates with cultured cells were washed with PBS, fixed with 2.5 % glutaraldehyde in PBS (1 h, 4 ºC), incubated with a series of ethanol solutions with increasing concentration (50 %, 70 %, 90 %, and 100 %) for dehydration, and dried overnight at RT. The dried substrates were mounted on the SEM pins, sputter-coated with gold (1 nm) and analyzed in a high-resolution field emission scanning electron microscope AIRIGA® (Zeiss).

2.7 Statistics. All reported data were obtained from three independent experiments (n=3) with gradients duplicates. To facilitate the analysis and data presentation, the gradients were divided into 10 equisized areas defined as positions 1-10. At least 3 regions were analyzed per each area. Data failed Levene's test for equality of variances at $p < 0.05$. The non-parametric Kruskal-Wallis test was used to determine statistical differences between the studied conditions (gold, HA, CD44 block, and RHAMM block) with a 95% confidence level. Multi-comparisons were tested using Benjamini and Hochberg *p*-adjusting method. Data processing, graphical representation, and statistical analysis were performed using RStudio (Version 1.2.5042).

3. Results and Discussion

Molecular gradients are commonly observed in biological systems. As an example, cells create gradients by secreting biomolecules that diffuse in the ECM. These gradients are temporally and spatially controlled and determine the cellular identity and fate.[31] They are critical for different physiological and pathological processes, including inflammation, wound healing, and cancer.[31] HA is a main component of the ECM that supports the normal cellular function. [1] However, in breast cancer, HA homeostasis is altered, resulting in accumulation of low molecular weight HA and formation of local gradients that play an important role in cancer.[32, 33] Thus, studies of cellular response to gradients of HA oligomers are of utmost interest for revealing mechanistic insights in HA-associated carcinogenesis and identifying possible molecular targets. Previous studies have

demonstrated that soluble low molecular weight HA has a chemoattractant effect (Dunn chamber assay) and promotes the directional migration of MDA-MB-231 and MDA-MB-486 cells.[34] However, either at the cell membrane or in the ECM, HA is partially immobilized by interactions with hyaluronan synthases (HAS), and other ECM components. To better mimic this scenario, hydrogel HA gradients have been developed to screen the cell behavior.[35-37] In this model, the gradient in HA content is concomitant with alterations in hydrogel mechanical properties, and it is not clear whether the cell response is triggered by HA-activated signaling pathways or mechanosensing. Recently, we have developed continuous HA gradients by surface immobilization of end-on thiolated HA (4.8 kDa) on gold gradients formed *via* diffusional deposition of colloidal nanoparticles (Fig. 1A1-3).[38]

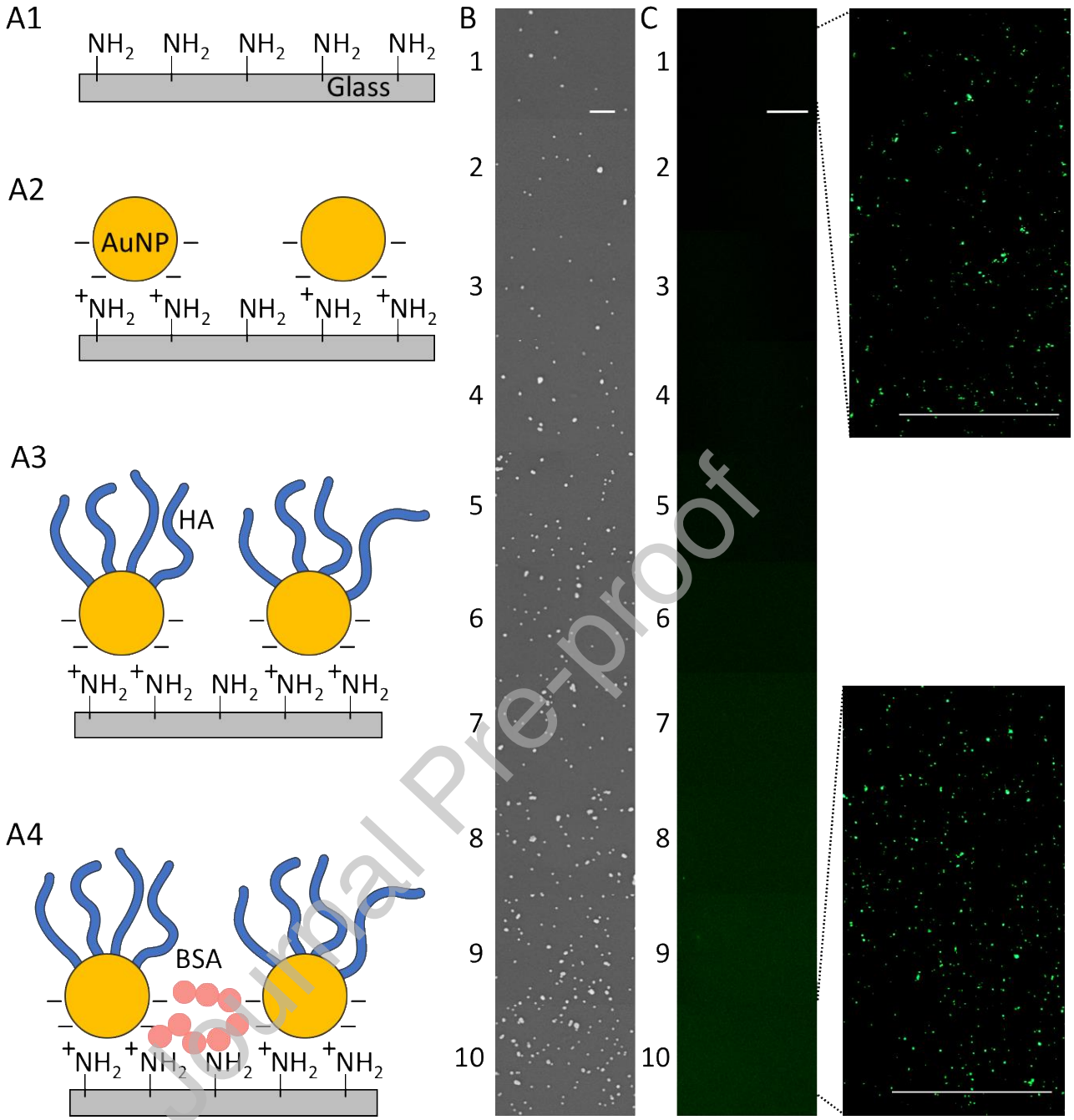

Figure 1. Preparation of hyaluronan gradients. (A) Schematic presentation of different experimental steps in the preparation of the gradients: (A1) amination of the substrates, (A2) electrostatic deposition of gold nanoparticles (AuNP), (A3) functionalization of the gold nanoparticles with thiolated hyaluronan (HA), and (A4) passivation of unfunctionalized surface with bovine serum albumin (BSA); **(B)** Representative scanning electron microscopy images of substrate surface along the gradient showing different density of the deposited gold nanoparticles, scale bar = 200 nm; **(C)** Representative fluorescence microscopy images showing the gradients used in this study after staining with Wheat germ agglutinin (WGA) Alexa Fluor® 488 conjugate, scale bar = 100 μm for the gradient and 500 μm for the magnified individual images at position 1 and 10. The respective quantification of the fluorescent intensity along the gradient is provided in Fig. S2 (SI).

This approach allows a relevant biofunctional presentation of HA since its main chain and functional groups are preserved. Herein, we used the same procedure to prepare HA gradients but after the HA deposition, the substrates were passivated with bovine serum albumin – a protein that does not bind HA and prevents cell adhesion (Fig. 1A4).[39, 40] As a result, we obtained gradients that have only one surface-exposed component for interaction with cells, *i.e.* HA whose bioactivity is preserved as demonstrated by binding with fluorescent-labeled wheat germ agglutinin (Figs. 1C, S1).[41]

3.1 CD44 and RHAMM expression by breast cancer cell lines.

CD44 and RHAMM interactions play a critical role in invasive breast cancer cells.[42] We used two breast cancer cell lines MDA-MB-231 (basal mesenchymal, triple-negative) and Sk-Br-3 (HER2-OE) [43, 44] with different aggressiveness and expression of CD44 and RHAMM.[5, 38, 45] The expression of these receptors was confirmed by immunocytochemistry (total expression) and flow cytometry (expression at the cell surface). The immunostaining showed that the two cell lines have similar expression of RHAMM but differ by the CD44 expression: MDA-MB-231 cells have a high CD44 expression, while Sk-Br-3 cells express less CD44 as shown by the faint staining (Fig. 2A). Because the recognition of extracellular HA occurs in the pericellular space, the expression of RHAMM and CD44 at the cell surface is consequential for cells/HA interactions. The results from the flow cytometry (Fig. 2B, characterization was performed without cell permeabilization) showed that the MDA-MB-231 cells are CD44 positive, while Sk-Br-3 cells are CD44 negative with only 10% of these cells exhibiting a basal CD44 expression at the cell surface. An opposite trend was observed for RHAMM expression – 40% of the Sk-Br-3 cells were positive for cell-surface RHAMM, while only 5% of the MDA-MB-231 cells were RHAMM positive but this population

express RHAMM at high levels. Therefore, the selected cell models have distinct phenotypes with MDA-MB-231 being CD44++/RHAMM+ and Sk-Br-3 CD44–/RHAMM++.

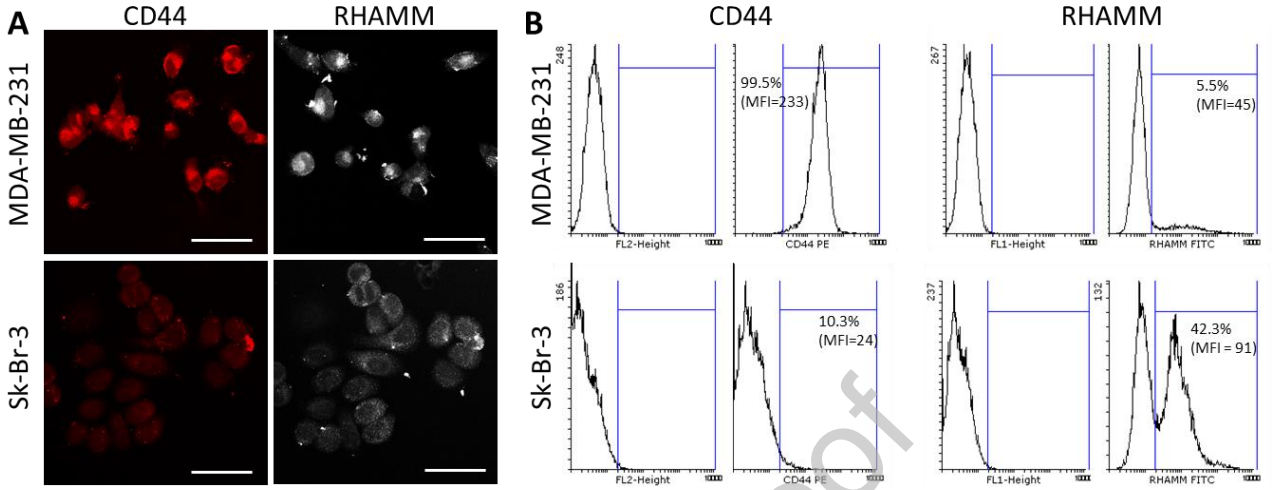

Figure 2. CD44 and RHAMM expression in MDA-MB-231 and Sk-Br-3 cells. **(A)** Confocal microscopy images of immunostained cells displaying the total expression of CD44 (red) and RHAMM (white) by the studied cells, scale bar = 50 μm; **(B)** Characterization of non-permeabilized cells by flow cytometry showing quantitative data for the CD44 and RHAMM expressed on the cells surface.

3.2 HA affects the adhesion of breast cancer cells

We observed a significant increase (p<0.005) of the cells adherent to the HA-functionalized gradients when compared to the control substrates (unfunctionalized gold gradients, Fig. 3A). The increase was bigger for Sk-Br-3 than for MDA-MB-231 (Fig. 3A). These results suggest HA-induced adhesion, *e.g.* through interaction with hyaladherins expressed at the cell surface, such as CD44 and RHAMM.[1, 46, 47]

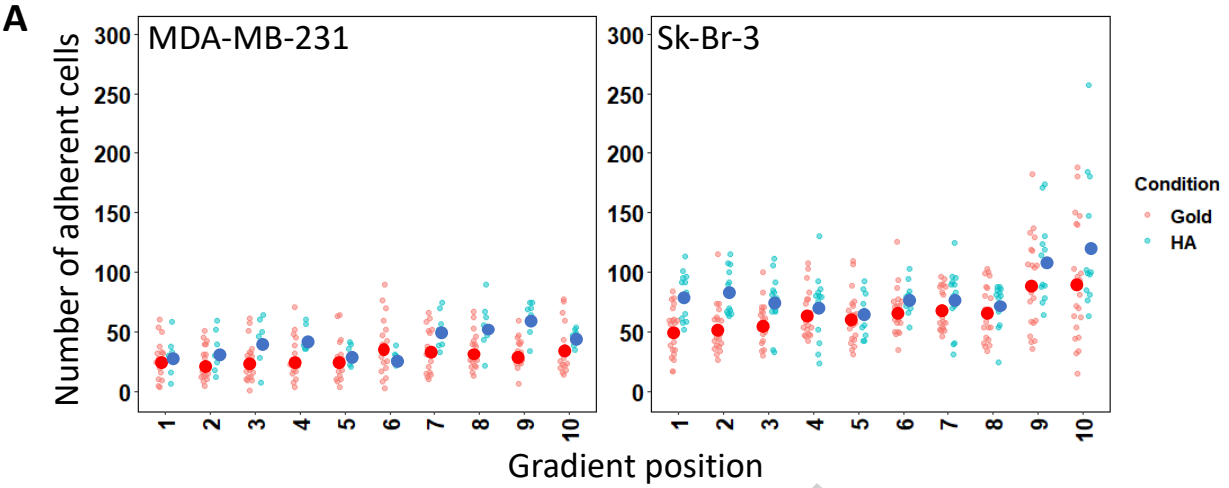

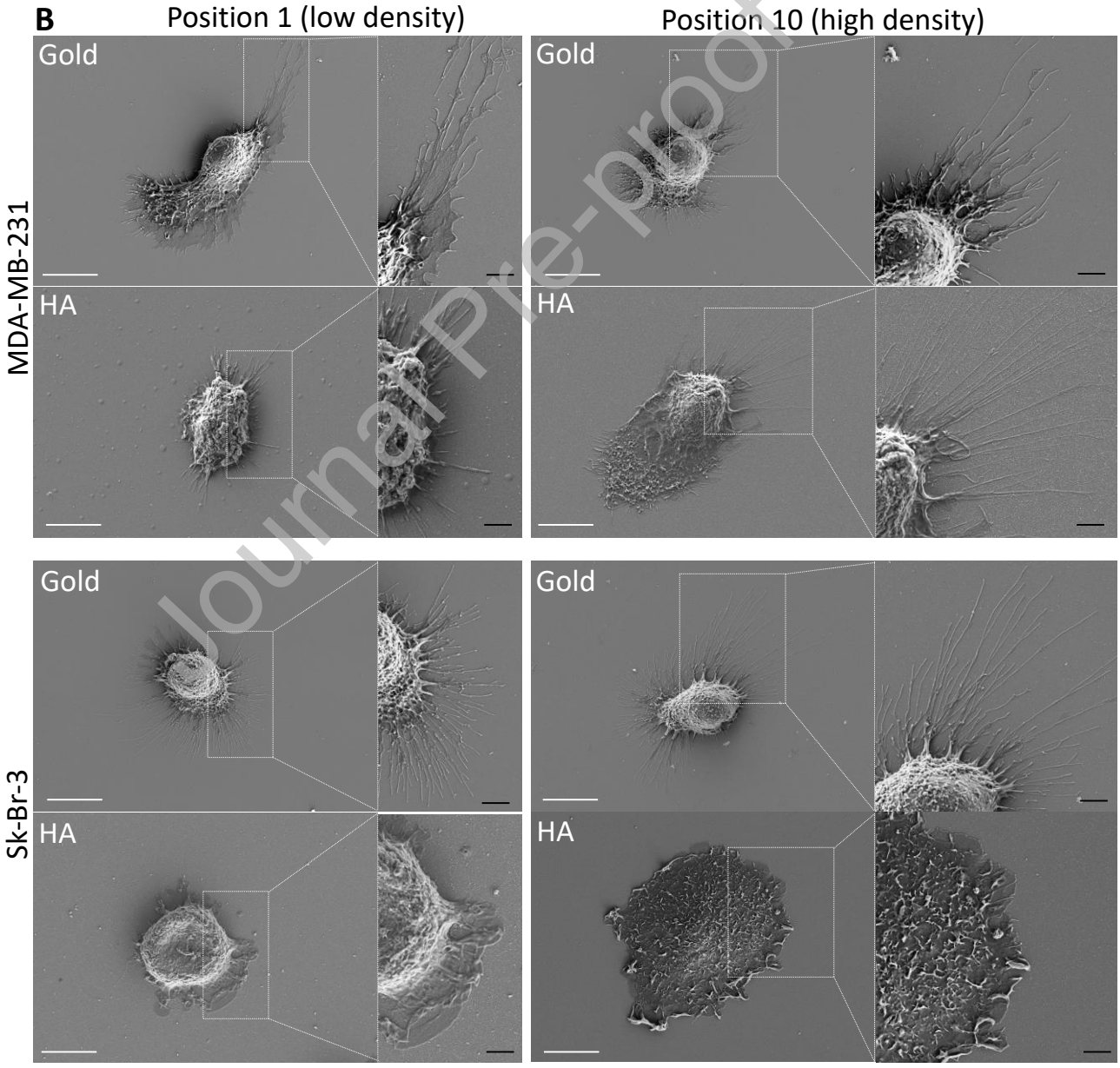

Figure 3. Adhesion of MDA-MB-231 and Sk-Br-3 cells to gold and HA gradients. (A) Number of adherent cells on gold (control) and HA gradients. Data for individual cells are presented as small points and big circles correspond to the mean values. Data sets for HA gradients are statistically significant from the control gradients (p<0.005, n=3). **(B)** Representative scanning electron microscopy images of breast cancer cells adherent to low- and high-density regions of HA gradients. White scale bar = 10 μm, black scale bar = 2.5 μm. The gradient density increases from position 1 to 10. Supplementary images are provided in Fig. S3 (SI).

The morphology of the cells adherent to HA gradients was evaluated by scanning electron microscopy (SEM, Figs. 3B and S3). On the passivated gold gradients, we observed spherical cells with numerous transient filopodia pointing in all directions consistent with the substrate exploring function of these protrusions. Cells on HA gradients were spread and with different morphology: Sk-Br-3 cells were round-shaped, while a spindle-like morphology was observed for MDA-MB-231 cells. These shapes were preserved along the HA gradient (Fig. S3) but we observed differences in the formed protrusions. In Sk-Br-3 cells the transient filopodia disappear completely in favor of lamellipodia, while MDA-MB-231 cells were polarized with parallel filopodia at the front edge (Figs. 3B and S3), *i.e.* a morphology typical for migrating cells. Of note, more and longer filopodia are visible for the MDA-MB-231 cells at higher HA density (Fig. S3). This result agrees with recent data that correlates an increased secretion of HA to the pericellular space of breast cancer cells with filopodial growth.[38, 48]

3.3 HA gradient modulates the expression of CD44 and RHAMM of breast cancer cells.

The bidirectional communication between cancer cells and their ECM results in a dynamic remodeling of the local cell environment, which in turn favors cancer progression.[49] Herein, we investigated the impact of the HA density on the behavior of breast cancer cells. The primary HA receptors, CD44 and RHAMM, are expected to be responsive towards changes in HA content.

Indeed, we observed a significant (p<0.005) increase of the CD44 expression for MDA-MB-231 cells (CD44++) adherent on HA gradients when compared to the control. Additionally, the CD44 expression was dependent on the HA density: higher HA density promoted CD44 expression by the MDA-MB-231 cells (Fig. 4A).

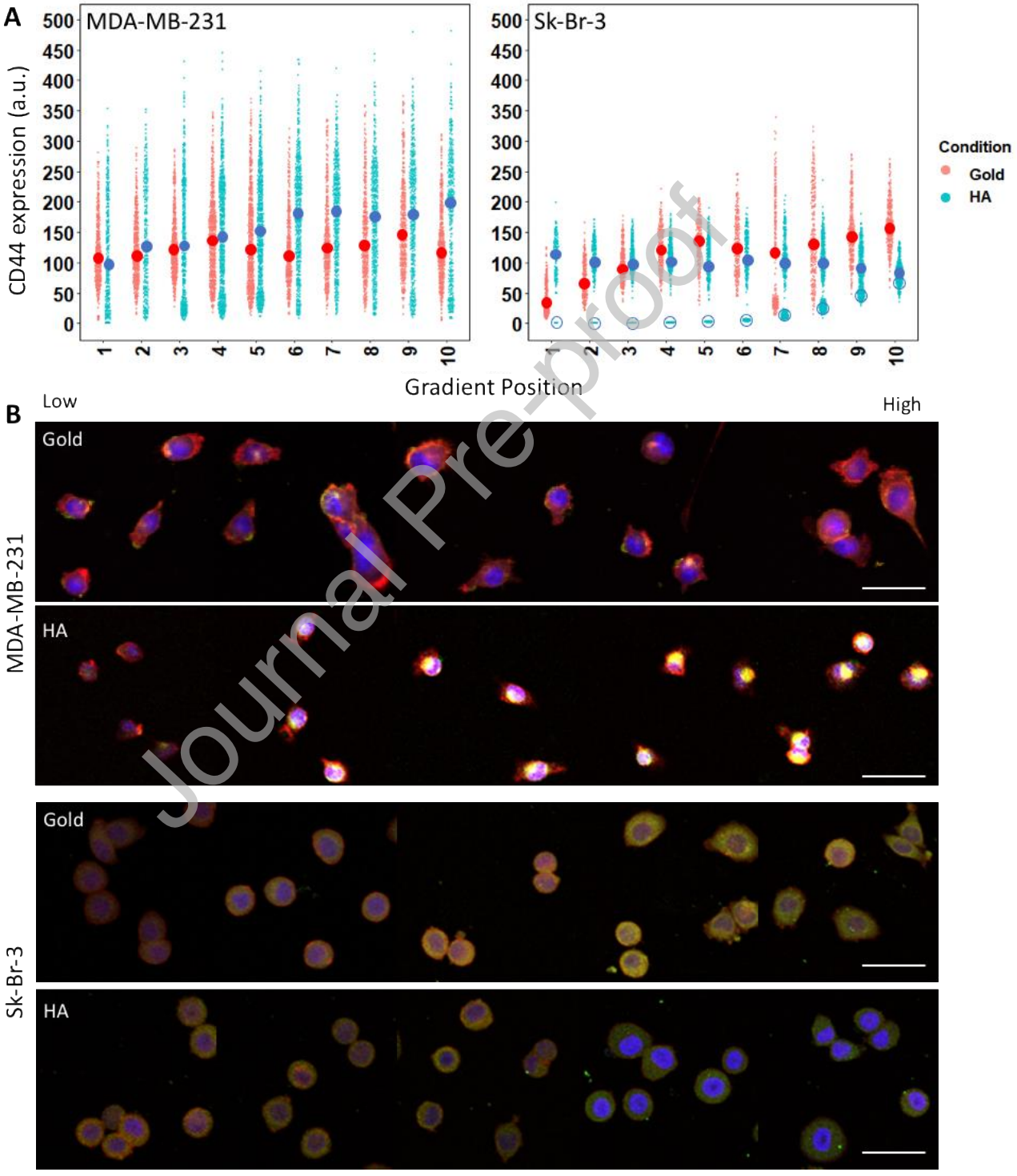

Figure 4. Expression of CD44 in response to HA density. (A) Graphical representation of CD44 expression by MDA-MB-231 and Sk-Br-3 cells seeded on gold and HA gradient (24 h of culture). Data for individual cells are presented as small points and big circles show the mean values. Trends for HA gradients are statistically significant from the control gradients (p<0.005, n=3). **(B)** Representative fluorescence microscopy images of breast cancer cells seeded on gold and HA gradient. Color code: CD44 (green), actin is stained with phalloidin (red), and the nuclei were counterstained with DAPI (blue), scale bar = 50 μm. Gradient density increases from position 1 to position 10.

Moreover, colocalization of CD44 and actin was observed (Fig. 4B) confirming the well-known involvement of HA/CD44 signaling in the cytoskeleton remodeling. Interesting results were obtained for the CD44 expression in Sk-Br-3 cells: we observed an increased CD44 expression along the gold gradient, indicating that these cells are sensitive to changes in the nanotopography introduced by the gold nanoparticles (Fig. 4A). The functionalization of the gold gradients with HA abolished this response and similar averaged CD44 expression was determined along the HA gradient. This result is indicative that the roughness introduced by the deposition of the gold nanoparticles is hidden after functionalization with HA and does not influence the cell response. Of note, the used method/platform allowed the distinction of Sk-Br-3 populations with different CD44 expression: one population that has the same average expression of this protein along the whole gradient (Fig. 4A, Sk-Br-3, filled blue circles) and a second population that is responsive to HA density (Fig. 4A, Sk-Br-3, contoured blue circles) and has low CD44 expression at low HA density (positions 1-6 of the HA gradient), which gradually increases upon augmentation of the HA density (positions 7-10). This result shows that besides the low CD44 expression, Sk-Br-3 cells use CD44 signaling to respond to HA density, although the activated pathway(s) might be different from the one(s) of MDA-MB-231 cells. The dispersal pattern of CD44 in the cytoplasm (Fig. 4B) supports such difference – in MDA-MB-231, CD44 is mainly observed around the nucleus while in Sk-Br-3 its distribution is even through all cytoplasm.

The effect of HA density was more pronounced for RHAMM expression (Fig. 5). When seeded on gold gradients, a higher average expression of RHAMM was observed for MDA-MB-231 cells than for Sk-Br-3 cells and no significant changes were determined along the gradient. Significantly higher (p<0.005) RHAMM expression was measured for cells seeded on HA gradients (Fig. 5A).

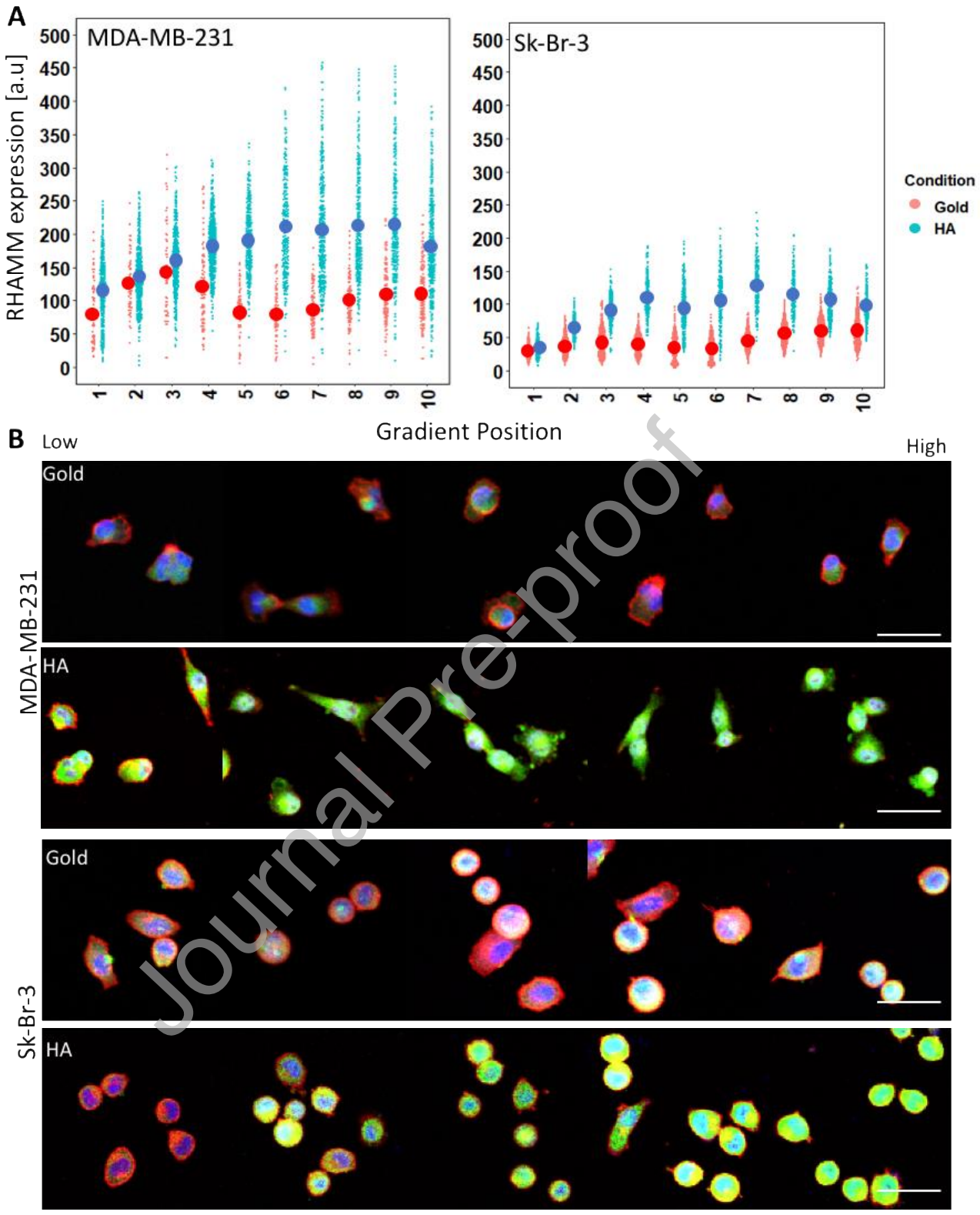

Figure 5. Expression of RHAMM by MDA-MB-231 and Sk-Br-3 breast cancer cells on gold and HA gradients. (A) Graphical representation of RHAMM expression by breast cancer cells along the gradients, small dots correspond to data for individual cells and the big dots are the mean values; trends for HA gradients are significantly different from the respective controls (p<0.005, n=3). **(B)** Representative fluorescence microscopy images of breast cancer cells interacting with gold and HA gradients. RHAMM is shown in green;

actin and nucleus were counterstained with phalloidin (red) and DAPI (blue), respectively, scale bar = 50 μm. HA density increases from position 1 to position 10.

Moreover, this increase was in a function of HA density, *i.e.* MDA-MB-231 and Sk-Br-3 cells adherent to gradient areas with higher HA density expressed more RHAMM. Despite different expression of HA receptors at the surface, MDA-MB-231 and Sk-Br-3 cells have a similar response to HA gradient. The expression of HA receptors by these cell lines changes upon interaction with HA gradients and both become CD44+/RHAMM++ (Fig. 4 and Fig. 5). This result demonstrates the importance of the tumor environment in potentiating pro-tumorigenic phenotypes. It agrees with previous reports about possible mechanisms inducing such response that can be RHAMM-mediated in the case of RHAMM++ cells (*e.g.* Sk-Br-3, mesenchymal progenitor cells)[5, 24] for which RHAMM can either act as a major receptor for HA binding (this is the case of non-adherent and newly attached cells) or function in synergism with CD44.[24] Our results showed major overexpression of RHAMM rather than CD44 for both cell lines, suggesting that RHAMM is a central receptor mediating the changes in HA content in the cell microenvironment. The central role of RHAMM in mediating pericellular HA changes has already been reported for RHAMM+ cancer subpopulations that were found to establish a migration front and promote peripheral and lymphatic invasion and metastasis in aggressive breast and colorectal cancers[50, 51].

3.4 CD44 and RHAMM redundancy on HA recognition.

To confirm the CD44 and RHAMM involvement in HA recognition, we performed activity blocking experiments (using neutralization antibodies) for MDA-MB-231 cells that have a more pronounced response to HA density. CD44 blocking resulted in a significant decrease in the expression of this receptor ($p<0.005$, Fig. 6A green) and upregulation of RHAMM ($p<0.005$, Fig. 6B green).

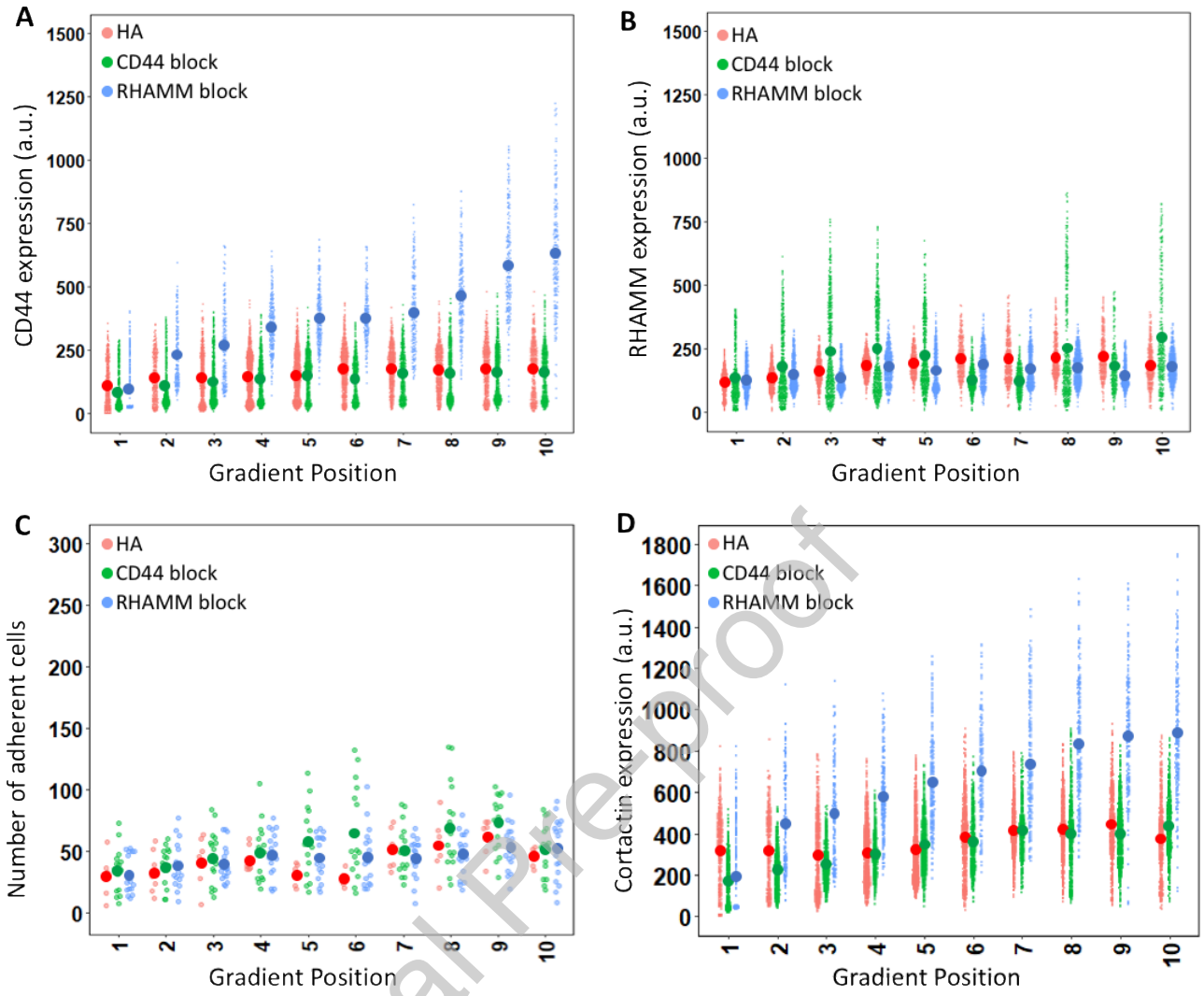

Figure 6. Characterization of MDA-MB-231 cells treated with blocking activity antibodies. (A) CD44 and **(B)** RHAMM expression by MDA-MB-231 cells seeded on HA gradients (controls) and treated with a blocking activity antibody against CD44 or RHAMM; trend for control is significantly different from RHAMM block (p<0.005, n=3). **(C)** Number of adherent cells on HA gradients before (controls) and after treatment with blocking activity antibody against CD44 and RHAMM. **(D)** Cortactin expression by MDA-MB-231 cells seeded on HA gradients and treated with an antibody against CD44 or RHAMM: trend for control is significantly different (p<0.005, n=3) from RHAMM and CD44 block; representative fluorescent microscopy images for cortactin expression are provided in Fig. S4 (SI). Small dots represent data for individual cells and the big dots are the mean values. HA density increases from position 1 to position 10.

When RHAMM was blocked instead, we observed RHAMM downregulation (p<0.005, Fig. 6B blue) and CD44 upregulation (p<0.005, Fig. 6A blue), which depends on the HA density. These results clearly demonstrate the redundancy of CD44 and RHAMM previously reported by us (*in*

vitro, [5]) and others (*in vivo* by knocking-out and knocking-down the CD44 gene [52-54]) and agree with the previously proposed compensatory mechanism between CD44 and RHAMM. Furthermore, we found a significantly higher number of adhered MDA-MB-231 cells after treatment with CD44 blocking antibody ($p<0.005$) but not for cells treated with RHAMM blocking antibody (Fig. 6C), *i.e.* the higher number of adherent cells correlates with the increase of RHAMM expression, confirming again that this receptor plays a fundamental role on HA binding.

We further investigated the impact of this compensatory mechanism on HA-induced protumorigenic signaling by evaluating the cortactin expression - a downstream effector common to CD44 and RHAMM mediated signaling.[55-61] Cortactin is a cytoskeletal protein involved in the formation of invadopodia and cell migration.[62, 63] It is a well-known transcriptional target of HA signaling transduced by interaction with CD44.[63, 64] We observed relatively high cortactin expression for the MDA-MB-231 cells seeded on HA gradients (Fig. 6D red). This expression increases along the gradient, indicating an HA-mediated response. The CD44 blocking did not significantly affect the cortactin expression by MDA-MB-231 cells (Fig. 6D green *vs.* red). On the other hand, the RHAMM blocking resulted in a significant increase of cortactin along the gradient ($p<0.005$, Fig. 6D blue *vs.* red) and the tendency was very similar to the observed for CD44 expression upon RHAMM blocking (Fig. 6A blue vs 6D blue). These results demonstrate that RHAMM and CD44 compensate each other in cortactin downstream signaling: RHAMM blocking evokes CD44 overexpression (as shown in Fig. 6A) and the overexpressed CD44 activates cortactin signaling cascade, *i.e.*, the increased expression of cortactin upon RHAMM blocking shows that cells still respond to the HA gradient by the present receptor – CD44, and this is proof for molecular redundancy between RHAMM and CD44.

Conclusions

During the last years, significant efforts have been devoted to HA-CD44 targeting in the context of cancer treatment. Such efforts include the use of anti-CD44 antibodies, inhibitory peptides, and siRNA/shRNA methodologies and are limited to CD44 without providing data for RHAMM.[65-75] Herein we have analyzed thousands of cells in a high-throughput manner and show a major role of RHAMM in HA recognition, *i.e.* in tunning the cell sensitivity towards its microenvironment. Our results demonstrate that cells with high surface expression of RHAMM are more sensitive to HA density. Such RHAMM overexpression can be phenotypic (native) or acquired upon CD44 blocking – conditions at which RHAMM is recruited to compensate CD44 in protumoregnic signaling. We also demonstrate that upon increasing of HA, both CD44 and RHAMM are recruited and protrusions are formed - these are essential steps in forming migration fronts.

Declaration of interests

The authors declare that they have no known competing financial interests or personal relationships that could have appeared to influence the work reported in this paper.

Acknowledgments

The authors thank the Portuguese FCT and FSE (Grants no: SFRH/BD/114847/2016, PTDC/NAN-MAT/28468/2017) and EU (Grant no: 668983-Forecast) for providing financial support to this project.

References:

[1] I. Caon, B. Bartolini, A. Parnigoni, E. Caravà, P. Moretto, M. Viola, E. Karousou, D. Vigetti, A. Passi, Revisiting the hallmarks of cancer: The role of hyaluronan, Semin. Cancer Biol. 62 (2020) 9-19.

[2] Y. Li, L. Li, T.J. Brown, P. Heldin, Silencing of hyaluronan synthase 2 suppresses the malignant phenotype of invasive breast cancer cells, Int. J. Cancer 120(12) (2007) 2557-2567.

[3] B. Bernert, H. Porsch, P. Heldin, Hyaluronan synthase 2 (HAS2) promotes breast cancer cell invasion by suppression of tissue metalloproteinase inhibitor 1 (TIMP-1), J. Biol. Chem. 286(49) (2011) 42349-42359.

[4] H. Koyama, T. Hibi, Z. Isogai, M. Yoneda, M. Fujimori, J. Amano, M. Kawakubo, R. Kannagi, K. Kimata, S.i. Taniguchi, Hyperproduction of hyaluronan in neu-induced mammary tumor accelerates angiogenesis through stromal cell recruitment: possible involvement of versican/PG-M, Am. J. Pathol. 170(3) (2007) 1086-1099.

[5] A.M. Carvalho, D. Soares da Costa, P.M.R. Paulo, R.L. Reis, I. Pashkuleva, Co-localization and crosstalk between CD44 and RHAMM depend on hyaluronan presentation, Acta Biomater. 119 (2021) 114-124.

[6] S. Liu, C. Cheng, Akt signaling is sustained by a CD44 splice isoform–mediated positive feedback loop, Cancer Res. 77(14) (2017) 3791-3801.

[7] B. Cieply, C. Koontz, S.M. Frisch, CD44S-hyaluronan interactions protect cells resulting from EMT against anoikis, Matrix Biol. 48 (2015) 55-65.

[8] T. Murai, Lipid raft-mediated regulation of hyaluronan–CD44 interactions in inflammation and cancer, Front. Immunol. 6 (2015) 420.

[9] S. Misra, S. Ghatak, B.P. Toole, Regulation of MDR1 expression and drug resistance by a positive feedback loop involving hyaluronan, phosphoinositide 3-kinase, and ErbB2, J. Biol. Chem. 280(21) (2005) 20310-20315.

[10] M.G. Slomiany, G.D. Grass, A.D. Robertson, X.Y. Yang, B.L. Maria, C. Beeson, B.P. Toole, Hyaluronan, CD44, and Emmprin regulate lactate efflux and membrane localization of monocarboxylate transporters in human breast carcinoma cells, Cancer Res. 69(4) (2009) 1293-1301.

[11] L.Y. Bourguignon, G. Wong, C. Earle, K. Krueger, C.C. Spevak, Hyaluronan-CD44 interaction promotes c-Src-mediated twist signaling, microRNA-10b expression, and RhoA/RhoC up-regulation,

leading to Rho-kinase-associated cytoskeleton activation and breast tumor cell invasion, J. Biol. Chem. 285(47) (2010) 36721-36735.

[12] S. Banerji, A.J. Day, J.D. Kahmann, D.G. Jackson, Characterization of a functional hyaluronan-binding domain from the human CD44 molecule expressed in Escherichia coli, Protein Expr. Purif. 14(3) (1998) 371-81.

[13] P. Teriete, S. Banerji, M. Noble, C.D. Blundell, A.J. Wright, A.R. Pickford, E. Lowe, D.J. Mahoney, M.I. Tammi, J.D. Kahmann, Structure of the regulatory hyaluronan binding domain in the inflammatory leukocyte homing receptor CD44, Mol. Cell 13(4) (2004) 483-496.

[14] H. Xu, K. Wu, Y. Tian, Q. Liu, N. Han, X. Yuan, L. Zhang, G.S. Wu, K. Wu, CD44 correlates with clinicopathological characteristics and is upregulated by EGFR in breast cancer, Int. J. Oncol. 49(4) (2016) 1343-1350.

[15] S. Han, T. Huang, W. Li, X. Wang, X. Wu, S. Liu, W. Yang, Q. Shi, H. Li, F. Hou, Prognostic value of CD44 and its isoforms in advanced cancer: a systematic meta-analysis with trial sequential analysis, Front. Oncol. 9 (2019) 39.

[16] B. Yang, B.L. Yang, R.C. Savani, E.A. Turley, Identification of a common hyaluronan binding motif in the hyaluronan binding proteins RHAMM, CD44 and link protein, EMBO J. 13(2) (1994) 286-296.

[17] J.M. Song, J. Im, R.S. Nho, Y.H. Han, P. Upadhyaya, F. Kassie, Hyaluronan-CD44/RHAMM interaction-dependent cell proliferation and survival in lung cancer cells, Mol. Carcinog. 58(3) (2019) 321-333.

[18] F. Chen, X.Q. Zhu, J. Zheng, T.T. Xu, K. Wu, C.H. Ru, RHAMM regulates the growth and migration of lung adenocarcinoma A549 cell line by regulating Cdc2/CyclinB1 and MMP9 genes Running title: RHAMM regulates the growth of lung adenocarcinoma cells, Math. Biosci. Eng. 17(3) (2020) 2150-2163.

[19] K. Kouvidi, A. Berdiaki, M. Tzardi, E. Karousou, A. Passi, D. Nikitovic, G.N. Tzanakakis, Receptor for hyaluronic acid- mediated motility (RHAMM) regulates HT1080 fibrosarcoma cell proliferation via a beta-catenin/c-myc signaling axis, Biochim. Biophys. Acta Gen. Subj. 1860(4) (2016) 814-824.

[20] V. Mele, L. Sokol, V.H. Kolzer, D. Pfaff, M.G. Muraro, I. Keller, Z. Stefan, I. Centeno, L.M. Terracciano, H. Dawson, I. Zlobec, G. Iezzi, A. Lugli, The hyaluronan-mediated motility receptor RHAMM promotes growth, invasiveness and dissemination of colorectal cancer, Oncotarget 8(41) (2017) 70617-70629.

[21] M. Mascaro, M.A. Pibuel, S.L. Lompardia, M. Diaz, E. Zotta, M.I. Bianconi, N. Lago, S. Otero, G. Jankilevich, E. Alvarez, S.E. Hajos, Low molecular weight hyaluronan induces migration of human choriocarcinoma JEG-3 cells mediated by RHAMM as well as by PI3K and MAPK pathways, Histochem. Cell Biol. 148(2) (2017) 173-187.

[22] C. Tolg, J.B. McCarthy, A. Yazdani, E.A. Turley, Hyaluronan and RHAMM in wound repair and the "cancerization" of stromal tissues, Biomed. Res. Int. 2014 (2014) 103923.

[23] M. Veiseh, D.H. Kwon, A.D. Borowsky, C. Tolg, H.S. Leong, J.D. Lewis, E.A. Turley, M.J. Bissell, Cellular heterogeneity profiling by hyaluronan probes reveals an invasive but slow-growing breast tumor subset, Proc. Natl. Acad. Sci. USA 111(17) (2014) E1731-E1739.

[24] M. Veiseh, S.J. Leith, C. Tolg, S.S. Elhayek, S.B. Bahrami, L. Collis, S. Hamilton, J.B. McCarthy, M.J. Bissell, E. Turley, Uncovering the dual role of RHAMM as an HA receptor and a regulator of CD44 expression in RHAMM-expressing mesenchymal progenitor cells, Front. Cell Dev. Biol. 3 (2015) 63.

[25] S. Nedvetzki, E. Gonen, N. Assayag, R. Reich, R.O. Williams, R.L. Thurmond, J.-F. Huang, B.A. Neudecker, F.-S. Wang, E.A. Turley, RHAMM, a receptor for hyaluronan-mediated motility, compensates for CD44 in inflamed CD44-knockout mice: a different interpretation of redundancy, Proc. Natl. Acad. Sci. USA 101(52) (2004) 18081-18086.

[26] C. Tolg, S.R. Hamilton, K.-A. Nakrieko, F. Kooshesh, P. Walton, J.B. McCarthy, M.J. Bissell, E.A. Turley, Rhamm−/− fibroblasts are defective in CD44-mediated ERK1, 2 motogenic signaling, leading to defective skin wound repair, J. Cell Biol. 175(6) (2006) 1017-1028.

[27] A.M. Carvalho, R. Teixeira, R. Novoa-Carballal, R.A. Pires, R.L. Reis, I. Pashkuleva, Redox-responsive micellar nanoparticles from glycosaminoglycans for CD44 targeted drug delivery, Biomacromolecules 19(7) (2018) 2991-2999.

[28] S. Karrasch, M. Dolder, F. Schabert, J. Ramsden, A. Engel, Covalent binding of biological samples to solid supports for scanning probe microscopy in buffer solution, Biophys. J. 65(6) (1993) 2437-2446.

[29] S.U. Argekar, T.L. Kirley, D.W.J.J.o.M.R. Schaefer, Determination of structure-property relationships for 3-aminopropyltriethoxysilane films using x-ray reflectivity, J. Mat. Res. 28(8) (2013) 1118-1128.

[30] J. Kimling, M. Maier, B. Okenve, V. Kotaidis, H. Ballot, A. Plech, Turkevich method for gold nanoparticle synthesis revisited, J. Phys. Chem. B 110(32) (2006) 15700-15707.

[31] T.M. Keenan, A. Folch, Biomolecular gradients in cell culture systems, Lab on a chip 8(1) (2008) 34-57.

[32] T. Kettunen, H. Okuma, P. Auvinen, M. Sudah, S. Tiainen, A. Sutela, A. Masarwah, M. Tammi, R. Tammi, S. Oikari, Peritumoral ADC values in breast cancer: region of interest selection, associations with hyaluronan intensity, and prognostic significance, Eur. Radiol. 30(1) (2020) 38-46.

[33] E.A. Turley, D.K. Wood, J.B. McCarthy, Carcinoma cell hyaluronan as a "portable" cancerized prometastatic microenvironment, Cancer Res. 76(9) (2016) 2507-12.

[34] G. Tzircotis, R.F. Thorne, C.M. Isacke, Chemotaxis towards hyaluronan is dependent on CD44 expression and modulated by cell type variation in CD44-hyaluronan binding, J. Cell Sci. 118(21) (2005) 5119-5128.

[35] K. Pogoda, R. Bucki, F.J. Byfield, K. Cruz, T. Lee, C. Marcinkiewicz, P.A. Janmey, Soft substrates containing hyaluronan mimic the effects of increased stiffness on morphology, motility, and proliferation of glioma cells, Biomacromolecules 18(10) (2017) 3040-3051.

[36] A.D. Rape, M. Zibinsky, N. Murthy, S. Kumar, A synthetic hydrogel for the high-throughput study of cell–ECM interactions, Nat. Commun. 6(1) (2015) 1-9.

[37] E. Hachet, H.l.n. Van Den Berghe, E. Bayma, M.R. Block, R. Auzély-Velty, Design of biomimetic cell-interactive substrates using hyaluronic acid hydrogels with tunable mechanical properties, Biomacromolecules 13(6) (2012) 1818-1827.

[38] A.M. Carvalho, D. Soares da Costa, R.L. Reis, I. Pashkuleva, Influence of hyaluronan density on the behavior of breast cancer cells with different CD44 expression, Adv. Healthc. Mater. 11(4) (2022) e2101309.

[39] B.K.D. Ngo, M.A. Grunlan, Protein resistant polymeric biomaterials, ACS Macro Lett. 6(9) (2017) 992-1000.

[40] L.E. Dickinson, C.C. Ho, G.M. Wang, K.J. Stebe, S. Gerecht, Functional surfaces for high-resolution analysis of cancer cell interactions on exogenous hyaluronic acid, Biomaterials 31(20) (2010) 5472-5478.

[41] Y.-P. Hsu, X. Meng, M. VanNieuwenhze, Methods for visualization of peptidoglycan biosynthesis, Methods Microbiol. 43 (2016) 3-48.

[42] S.R. Hamilton, S.F. Fard, F.F. Paiwand, C. Tolg, M. Veiseh, C. Wang, J.B. McCarthy, M.J. Bissell, J. Koropatnick, E.A. Turley, The hyaluronan receptors CD44 and Rhamm (CD168) form complexes with ERK1, 2 that sustain high basal motility in breast cancer cells, J. Biol. Chem. 282(22) (2007) 16667-16680.

[43] T. Sørlie, C.M. Perou, R. Tibshirani, T. Aas, S. Geisler, H. Johnsen, T. Hastie, M.B. Eisen, M. Van De Rijn, S.S. Jeffrey, Gene expression patterns of breast carcinomas distinguish tumor subclasses with clinical implications, Proc. Natl. Acad. Sci. USA 98(19) (2001) 10869-10874.

[44] T. Sorlie, R. Tibshirani, J. Parker, T. Hastie, J.S. Marron, A. Nobel, S. Deng, H. Johnsen, R. Pesich, S. Geisler, J. Demeter, C.M. Perou, P.E. Lønning, P.O. Brown, A.-L. Børresen-Dale, D. Botstein, Repeated observation of breast tumor subtypes in independent gene expression data sets, Proc. Natl. Acad. Sci. USA 100(14) (2003) 8418-8423.

[45] W. Li, H. Ma, J. Zhang, L. Zhu, C. Wang, Y. Yang, Unraveling the roles of CD44/CD24 and ALDH1 as cancer stem cell markers in tumorigenesis and metastasis, Sci. Rep. 7(1) (2017) 1-15.

[46] P.M. Witschen, T.S. Chaffee, N.J. Brady, D.N. Huggins, T.P. Knutson, R.S. LaRue, S.A. Munro, L. Tiegs, J.B. McCarthy, A.C. Nelson, Tumor cell associated hyaluronan-CD44 signaling promotes pro-tumor inflammation in breast cancer, Cancers 12(5) (2020) 1325.

[47] S. Reiprich, E. Hofbauer, S. Kiderlen, H. Clausen-Schaumann, W. Böcker, A. Aszódi, V. Schönitzer, Adhesive properties of the hyaluronan pericellular coat in hyaluronan synthases overexpressing mesenchymal stem cells, Int. J. Mol. Sci. 21(11) (2020) 3827.

[48] H. Kyykallio, S. Oikari, M. Bueno Álvez, C.J. Gallardo Dodd, J. Capra, K. Rilla, The density and length of filopodia associate with the activity of hyaluronan synthesis in tumor cells, Cancers 12(7) (2020) 1908.

[49] J. Winkler, A. Abisoye-Ogunniyan, K.J. Metcalf, Z. Werb, Concepts of extracellular matrix remodelling in tumour progression and metastasis, Nat. Commun. 11(1) (2020) 1-19.

[50] C. Wang, A.D. Thor, D. Moore, Y. Zhao, R. Kerschmann, R. Stern, P.H. Watson, E.A. Turley, The overexpression of RHAMM, a hyaluronan-binding protein that regulates ras signaling, correlates with overexpression of mitogen-activated protein kinase and is a significant parameter in breast cancer progression, Clin. Cancer Res. 4(3) (1998) 567-576.

[51] V.H. Koelzer, B. Huber, V. Mele, G. Iezzi, M. Trippel, E. Karamitopoulou, I. Zlobec, A. Lugli, Expression of the hyaluronan-mediated motility receptor RHAMM in tumor budding cells identifies aggressive colorectal cancers, Hum. Pathol. 46(11) (2015) 1573-1581.

[52] S. Misra, V.C. Hascall, R.R. Markwald, S. Ghatak, Interactions between hyaluronan and its receptors (CD44, RHAMM) regulate the activities of inflammation and cancer, Front. Immunol. 6 (2015) 201.

[53] H. Takano, S. Nakazawa, N. Shirata, S. Tamba, K. Furuta, S. Tsuchiya, K. Morimoto, N. Itano, A. Irie, A. Ichikawa, Involvement of CD44 in mast cell proliferation during terminal differentiation, Lab. Investig. 89(4) (2009) 446-455.

[54] W. Xiao, R. Zhang, A. Sohrabi, A. Ehsanipour, S. Sun, J. Liang, C.M. Walthers, L. Ta, D.A. Nathanson, S.K. Seidlits, Brain-mimetic 3D culture platforms allow investigation of cooperative effects of extracellular matrix features on therapeutic resistance in glioblastoma, Cancer Res. 78(5) (2018) 1358-1370.

[55] L.Y. Bourguignon, E. Gilad, K. Rothman, K. Peyrollier, Hyaluronan-CD44 interaction with IQGAP1 promotes Cdc42 and ERK signaling, leading to actin binding, Elk-1/estrogen receptor transcriptional activation, and ovarian cancer progression, J. Biol. Chem. 280(12) (2005) 11961-11972.

[56] S. McFarlane, C. McFarlane, N. Montgomery, A. Hill, D.J.J. Waugh, CD44-mediated activation of α5β1-integrin, cortactin and paxillin signaling underpins adhesion of basal-like breast cancer cells to endothelium and fibronectin-enriched matrices, Oncotarget 6(34) (2015) 36762-36773.

[57] D. Vigetti, M. Viola, E. Karousou, M. Rizzi, P. Moretto, A. Genasetti, M. Clerici, V.C. Hascall, G. De Luca, A.J.J.o.B.C. Passi, Hyaluronan-CD44-ERK1/2 regulate human aortic smooth muscle cell motility during aging, 283(7) (2008) 4448-4458.

[58] S. Zhang, M.C.Y. Chang, D. Zylka, S. Turley, R. Harrison, E.A. Turley, The Hyaluronan Receptor RHAMM Regulates Extracellular-regulated Kinase, Journal of Biological Chemistry 273(18) (1998) 11342-11348.

[59] C.L. Hall, L.A. Lange, D.A. Prober, S. Zhang, E.A. Turley, pp60(c-src) is required for cell locomotion regulated by the hyaluronanreceptor RHAMM, Oncogene 13(10) (1996) 2213-2224.

[60] C.L. Hall, C. Wang, L.A. Lange, E.A. Turley, Hyaluronan and the hyaluronan receptor RHAMM promote focal adhesion turnover and transient tyrosine kinase activity, The Journal of cell biology 126(2) (1994) 575-588.

[61] C. Wang, A.D. Thor, D.H. Moore, Y. Zhao, R. Kerschmann, R. Stern, P.H. Watson, E.A. Turley, The overexpression of RHAMM, a hyaluronan-binding protein that regulates ras signaling, correlates with overexpression of mitogen-activated protein kinase and is a significant parameter in breast cancer progression, 4(3) (1998) 567-576.

[62] A.M. Weaver, Cortactin in tumor invasiveness, Cancer letters 265(2) (2008) 157-166.

[63] L.W. Bourguignon, H. Zhu, L. Shao, Y.-W. Chen, CD44 interaction with c-Src kinase promotes cortactin-mediated cytoskeleton function and hyaluronic acid-dependent ovarian tumor cell migration, Journal of Biological Chemistry 276(10) (2001) 7327-7336.

[64] S. McFarlane, C. McFarlane, N. Montgomery, A. Hill, D.J. Waugh, CD44-mediated activation of α5β1-integrin, cortactin and paxillin signaling underpins adhesion of basal-like breast cancer cells to endothelium and fibronectin-enriched matrices, Oncotarget 6(34) (2015) 36762.

[65] G. Song, X. Liao, L. Zhou, L. Wu, Y. Feng, Z.C. Han, HI44a, an anti-CD44 monoclonal antibody, induces differentiation and apoptosis of human acute myeloid leukemia cells, Leukemia research 28(10) (2004) 1089-96.

[66] L. Jin, K.J. Hope, Q. Zhai, F. Smadja-Joffe, J.E. Dick, Targeting of CD44 eradicates human acute myeloid leukemic stem cells, Nature medicine 12(10) (2006) 1167-74.

[67] M. Tremmel, A. Matzke, I. Albrecht, A.M. Laib, V. Olaku, K. Ballmer-Hofer, G. Christofori, M. Héroult, H.G. Augustin, H. Ponta, V. Orian-Rousseau, A CD44v6 peptide reveals a role of CD44 in VEGFR-2 signaling and angiogenesis, Blood 114(25) (2009) 5236-44.

[68] A. Matzke, P. Herrlich, H. Ponta, V. Orian-Rousseau, A Five-Amino-Acid Peptide Blocks Met- and Ron-Dependent Cell Migration, Cancer research 65(14) (2005) 6105-6110.

[69] D. Peck, C.M. Isacke, Hyaluronan-dependent cell migration can be blocked by a CD44 cytoplasmic domain peptide containing a phosphoserine at position 325, Journal of cell science 111(11) (1998) 1595-601.

[70] B. Desai, T. Ma, J. Zhu, M.A. Chellaiah, Characterization of the expression of variant and standard CD44 in prostate cancer cells: Identification of the possible molecular mechanism of CD44/MMP9 complex formation on the cell surface, Journal of Cellular Biochemistry 108(1) (2009) 272-284.

[71] R.S. Piotrowicz, B.B. Damaj, M. Hachicha, F. Incardona, S.B. Howell, M. Finlayson, A6 Peptide Activates CD44 Adhesive Activity, Induces FAK and MEK Phosphorylation, and Inhibits the Migration and Metastasis of CD44-Expressing Cells, Molecular cancer therapeutics 10(11) (2011) 2072-2082.

[72] D.D. Boyd, S.-J. Kim, H. Wang, T.R. Jones, C.E. Gallick, A urokinase-derived peptide (A6) increases survival of mice bearing orthotopically grown prostate cancer and reduces lymph node metastasis, Am J Pathol 162(2) (2003) 619-626.

[73] M.E. Mummert, D.I. Mummert, L. Ellinger, A. Takashima, Functional roles of hyaluronan in B16-F10 melanoma growth and experimental metastasis in mice, Molecular cancer therapeutics 2(3) (2003) 295-300.

[74] C.P. Paul, P.D. Good, I. Winer, D.R. Engelke, Effective expression of small interfering RNA in human cells, Nature biotechnology 20(5) (2002) 505-8.

[75] S. Misra, V.C. Hascall, C. De Giovanni, R.R. Markwald, S. Ghatak, Delivery of CD44 shRNA/nanoparticles within cancer cells: perturbation of hyaluronan/CD44v6 interactions and reduction in adenoma growth in Apc Min/+ MICE, Journal of Biological Chemistry 284(18) (2009) 12432-46.

GA